
Modeling Temperature and Pressure Gradients During Cooling of Thin-Walled Cryogenic Targets

Introduction

High-quality targets must be provided to achieve successful results from OMEGA cryogenic experiments.¹ One type of target is a thin-walled polymer capsule with a fuel layer of solid deuterium (D_2) or deuterium/tritium (DT) ice, approximately $100\ \mu\text{m}$ thick, uniformly distributed on the inner wall of the capsule.² To create the fuel layer, the capsule is placed in a room-temperature pressure vessel and slowly pressurized, filling the capsule by permeation through the polymer wall.³ The capsule is slowly cooled to the critical point ($\sim 38.3\ \text{K}$ for D_2) to first liquefy the gas, and then further cooled to freeze it. The mass of ice is made uniform through layering techniques.⁴ Because of the capsules' fragile nature and the great amount of time required to fill them, the cooling process is a critical phase of operation for providing cryogenic targets.

The filling and cooling of the capsules takes place in the permeation cell. The permeation cell is a pressure vessel constructed of A-286, a high-strength Ni-based superalloy, which contains an insert bearing the capsules called the target rack. The permeation cell contains two parts: (1) an outer surface that carries the mechanical load designed to contain up to 1500 atm and (2) an inner surface that is the outer wall of the pressure vessel. This inner surface has a heater and silicon-diode temperature sensors bonded to it. The outer surfaces are actively cooled by helium gas at 8 K flowing through a tube wound around the outside of the permeation cell. The temperature inside the permeation cell is measured by silicon temperature sensors imbedded at various locations and is maintained by regulating the helium flow and the power to the heater on the core around the target rack. The capsules are fixed in "C-mounts" between four threads of spider silk and placed into the target rack, which is inserted into the center of the permeation cell.⁵ The target rack is designed to minimize free volume around the capsule and is constructed of high-conductivity copper to minimize temperature gradients.

This article presents the results of both a steady-state analysis and a transient analysis of the pressure differences across the wall of a thin-walled capsule during the cooling

process. The analyses were separated to quantify the effects that each phenomenon contributes. The steady-state contribution to the pressure difference arises from two sources: (1) the different thermal contractions of the materials that comprise the permeation cell and capsule and (2) the room-temperature volume of gas in the line connecting the permeation cell to the isolation valve. An optimum value for the room-temperature volume has been found that minimizes the burst and buckle pressures and allows for 1- and 3- μm -wall capsules to be filled. The transient analysis considered the pressure differences across the capsule wall that arise from temperature changes to the permeation cell. A 3- μm -wall capsule can withstand changes of 1 K at warmer temperatures, while a 1- μm -wall capsule should not be subjected to sudden temperature changes of more than 0.1 K. A cooling program that incorporates permeability at higher temperatures and safely maintains the capsule within the critical burst and buckle pressures allows the time to reach the frozen state to be reduced by over 30%.

Effect of Thermal Contraction and Room-Temperature Volume

Targets to be filled with D_2 or DT are held at room temperature while the pressure is raised at a slow, steady rate, typically to 1000 atm. The pressurization rate is based on the permeability of the capsule wall and its strength against buckling. To assure the capsule's survival, the pressurization rate is kept below P_{buckle}/τ , where P_{buckle} is the buckling pressure and τ is the permeation time constant. For a glow discharge polymer (GDP) capsule of 920- μm diameter with a 3- μm wall, $P_{\text{buckle}} \cong 1\ \text{atm}$ and $\tau \cong 30\ \text{s}$, which allows a 1000-atm fill in 11 h. It is assumed, for safety, that the fill proceeds 30% more slowly than the maximum rate. If the wall thickness is 1 μm , $P_{\text{buckle}} \cong 0.1\ \text{atm}$ and $\tau \cong 10\ \text{s}$, which requires 36 h for a similar fill. When the GDP capsules are fabricated, modifying the deposition conditions for the GDP⁶ can result in increased P_{buckle} along with higher permeability, which should allow slightly more rapid filling. After filling, a valve is closed, which isolates the permeation cell from the compressor, and the permeation cell is slowly cooled. The cooling proceeds slowly in order to (1) minimize thermal gradients in the permeation

cell and (2) allow some permeation through the capsule wall in response to a pressure differential that develops during the cooling process.

The pressure differential across the capsule wall arises partly because of a small room-temperature volume connected to the permeation cell, and partly because of differences in the thermal contraction between the polymer capsule wall and the metals of the permeation cell. The small room-temperature volume formed by the isolation valve and the tube connecting this valve to the permeation cell exists because of the unavailability of a suitable cryogenic valve. This room-temperature volume generates an external pressure on the capsule because the increasing density of the gas, as it cools, draws some of the less-dense room-temperature gas into the permeation cell. Simultaneously, the thermal contraction of both the polymer of the capsule wall, which is nearly four times greater than the contraction of the stainless steel of the permeation cell, and the copper of the target rack tends to create an excess internal pressure in the capsule.

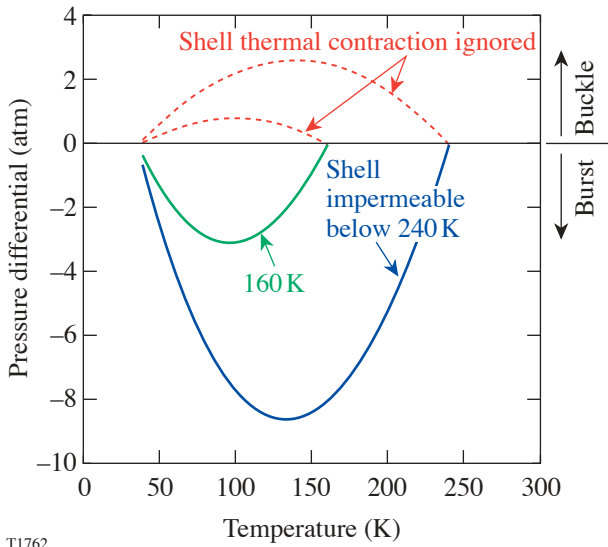
To assess these competing effects, the pressure across the capsule wall during the cooldown is calculated for various values of room-temperature volume. These calculations use the NIST equation of state for deuterium,⁷ which expresses pressure as a 24-term function of density and temperature. Starting with room-temperature volumes for the permeation cell, the copper target rack, and the small external volume, the molar content is calculated, assuming a 1000-atm fill. At each reduced temperature, the volumes of the cooled elements are recalculated based on the thermal contraction values for copper and stainless steel.⁸ The portion of the connecting tube between the room-temperature volume and the permeation cell that has a thermal gradient on it—one-quarter as large as the room-temperature volume—is treated as being part of the room-temperature volume. While varying the temperature of the permeation cell, the pressure and density in the cell are determined by solving three simultaneous equations: (1) conservation of the sum of the molar content of the permeation cell and the room-temperature volume, taking thermal contraction into account; (2) equating the pressure in the permeation cell with that in the room-temperature volume; and (3) applying the deuterium equation of state.

To calculate the pressure in the capsule during the cooldown, a temperature is arbitrarily selected below which the capsule is assumed to be impermeable. This strategy is justified by the sharp decrease in permeability with temperature generally exhibited by polymers, following the Arrhenius

relation. The activation energy for this process has not been measured for the GDP shell material, so the temperature at which the shell becomes effectively impermeable is unknown; however, comparison to polystyrene,⁹ which has a similar value of room-temperature permeability, suggests this temperature is in the range of 160 K to 240 K, depending on wall thickness and cooling rate. Within this temperature range, the permeation time constants of capsules with wall thicknesses of 1 to 3 μm range from 10 to 60 min. At lower temperatures, no significant permeation occurs with practical rates of cooling, such as 0.1 K/min. Vapor-deposited polyimide, which is less permeable,¹⁰ becomes effectively impermeable in the temperature range of 220 K to 290 K, if it is previously unstrained. The thermal contraction of GDP is estimated by scaling the polystyrene data⁹ with a contraction value measured for a GDP sample cooled from room temperature to 77 K. The length of this flat sample was found to decrease by 0.99% when immersed in liquid nitrogen, compared to 1.32% for the polystyrene data. To estimate the GDP contraction as a function of temperature, the polystyrene data are multiplied by 0.75, the ratio of the GDP value to the polystyrene value at 77 K.

The results of these calculations are shown in Figs. 94.50–94.53. In Fig. 94.50, it is seen that if the room-temperature volume is zero (i.e., if there was a cryogenically cooled isolation valve), a substantial bursting pressure is generated. It is also seen that if there was no shell contraction, the pressure differential generated would be external—a buckling pressure. Comparing Fig. 94.51 to Fig. 94.50, it is seen that adding a relatively small room-temperature volume of 0.3 cc changes the result from a strong bursting pressure to a strong buckling pressure. In Fig. 94.52, an effective compromise between these cases is shown. Reducing the warm volume to 0.11 cc yields a tolerable buckling pressure that a thin-walled capsule should survive and a similarly modest bursting pressure. This conclusion seems to hold regardless of what temperature in the range 160 K to 240 K best represents the effective point at which the capsule becomes impermeable. Other values of warm volume were tried, and 0.11 cc was found to be an optimum value. The volume actually achieved, however, after insertion of volume reducers is estimated to be 0.17 cc. Figure 94.53 plots the pressure differential across the capsule as a function of temperature for various temperatures at which the capsule could become impermeable. A positive pressure differential exceeding 1.5 atm develops, easily buckling a capsule with a 1- μm wall.

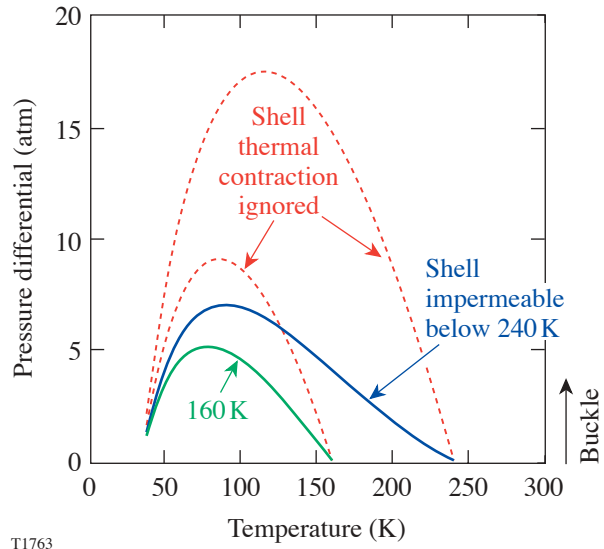
The expected buckling pressures shown in Fig. 94.53 for capsules with 1- μm and 3- μm wall thickness are calculated



T1762

Figure 94.50

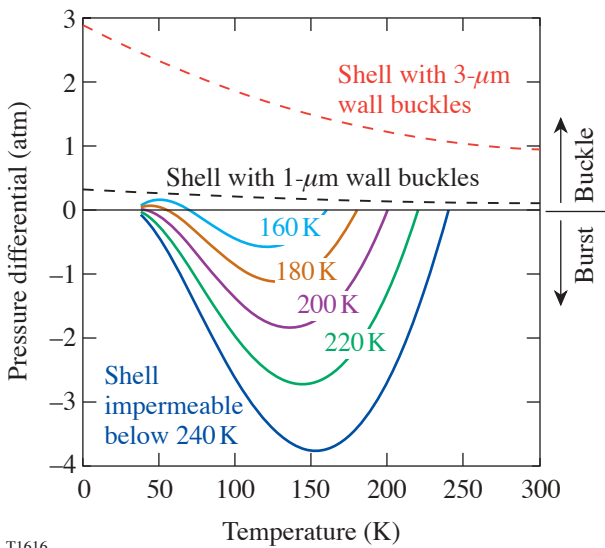
The calculated pressure differential across a capsule wall (assumed inelastic) is plotted for the case of zero room-temperature volume. The capsule is permeated with 1000 atm of D₂ and then cooled slowly to 25 K or lower. The dashed lines indicate the excess external pressure (buckling pressure) that would occur if thermal contraction of the permeation cell is taken into account, but not thermal contraction of the capsule. The solid lines include capsule contraction and show a large bursting pressure. If the capsule becomes impermeable at 240 K, a very large burst pressure is generated, while permeability at temperatures down to 160 K, followed by impermeability at lower temperatures, produces more-modest internal pressures.



T1763

Figure 94.51

The calculated pressure differential across a capsule wall is plotted for a realistic room-temperature volume of 0.3 cc and a permeation cell volume of 5 cc. The dashed lines ignore thermal contraction and the solid lines include it. An excess pressure external to the capsule arises that would cause any thin-walled capsule to buckle. An inelastic capsule is assumed. The room-temperature volume is reduced from this value by insertion of spacers.

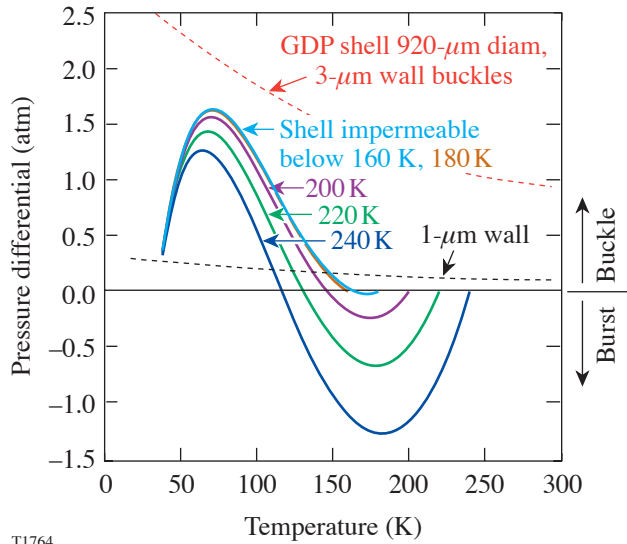


T1616

Figure 94.52

The calculated pressure differential across a capsule wall is plotted for a small value of room temperature volume for various temperatures at which the capsule could become impermeable. The dashed lines indicate the buckling pressure of capsules with 1- and 3- μ m walls. Reducing the room-temperature volume to 0.11 cc reduces the buckling pressure to a level that is survivable by an inelastic shell with a 1- μ m wall. While this volume appears optimal, it would be difficult to achieve such a small volume.

using values of Young’s modulus inferred from measuring the buckling pressures of a group of GDP capsules at various temperatures. It is found that Young’s modulus increases significantly upon cooling, reaching a value at 10 K of 2.5× the value at room temperature.



T1764

Figure 94.53
The calculated pressure differential across an inelastic capsule wall is plotted for an achievable room-temperature volume of 0.17 cc for various temperatures at which the capsule could become impermeable. The dashed lines show the buckling pressures for capsules with 1- and 3-μm walls. The thicker-walled capsules would survive, while the thinner-walled ones would not.

Effect of Shell Elasticity

The preceding calculations do not take into account the expansion or shrinkage of the capsule due to internal or external pressure. Taking into account dimensional change due to elasticity reduces the resulting differential pressure on the capsule wall,¹¹ rendering it less vulnerable to bursting or buckling. The calculations assume the capsule wall is perfectly spherical, uniform in thickness, and homogeneous. The fractional change in the radius *r* is given¹² by

$$\frac{\Delta r}{r} = \frac{r \Delta P(1 - \nu)}{2 E w}, \tag{1}$$

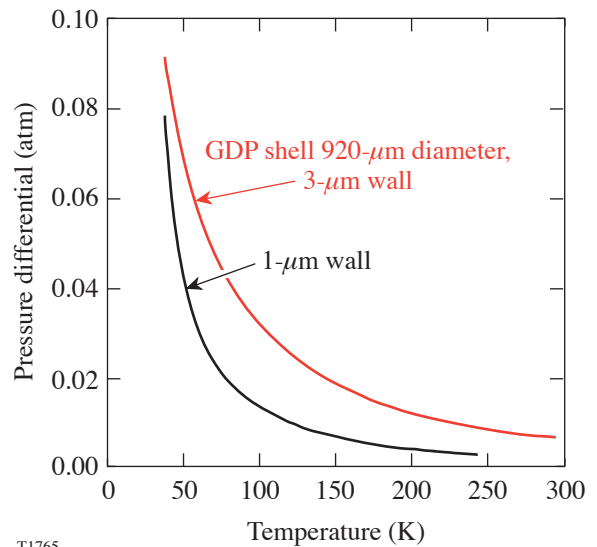
where ΔP is the pressure differential across the wall, ν is Poisson’s ratio of the capsule material (the polystyrene value, 0.35, is used here), E is Young’s modulus, and w is the wall thickness. While deuterium at the densities of a typical target

fill is far from an ideal gas, it is useful to consider the functional dependence of the pressure differential on elasticity for the ideal gas case. If a pressure differential ΔP_i is applied across a capsule wall, which thereupon undergoes elastic expansion or contraction, the final pressure differential is readily found to be, in the ideal gas case, for $\Delta r \ll r$,

$$\Delta P_f \cong \frac{\Delta P_i}{1 + (P + \Delta P_i) \frac{3r(1 - \nu)}{2 E w}}, \tag{2}$$

where P is the initial pressure inside and outside the capsule. This solution is useful as a check on the non-ideal-gas solution at its low-pressure limit.

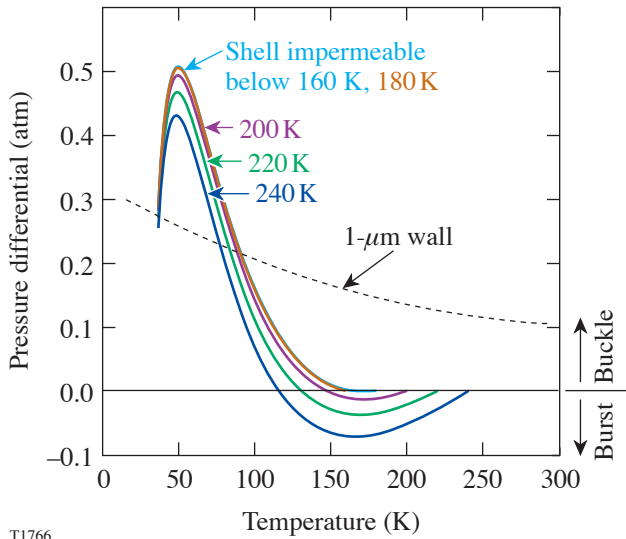
To calculate ΔP resulting from a change in the pressure external to the capsule for the non-ideal-gas case, Eq. (1) is solved by applying the deuterium equation of state along with the requirement that the molar content of the capsule is unchanged. The result, dependent on temperature and wall thickness, is shown in Fig. 94.54 for the case of a 0.1-atm change in the external pressure. Applying this method to the pressure differential that results from thermal contraction and a room-



T1765

Figure 94.54
Pressure differential across the wall of an elastic capsule (GDP) that has expanded or contracted due to a 0.1-atm change in external pressure. The capsule diameter is 920 μm, and the wall thickness is 1 or 3 μm. At such a high gas density (~25 mol/L), external pressure changes are substantially attenuated.

temperature volume, the data in Fig. 94.53 are transformed into Fig. 94.55. For a room-temperature volume of 0.17 cc, the maximum pressure differential is reduced from 1.6 atm to 0.5 atm but is still enough to buckle a shell with a 1- μm wall. The buckling problem could be solved by reducing the warm volume to 0.11 cc or by adjusting thermal gradients in the permeation cell. These calculations, showing reduced vulnerability to failure due to capsule elasticity, assume the capsule is perfectly spherical and of uniform wall thickness, and have not been tested experimentally.



T1766

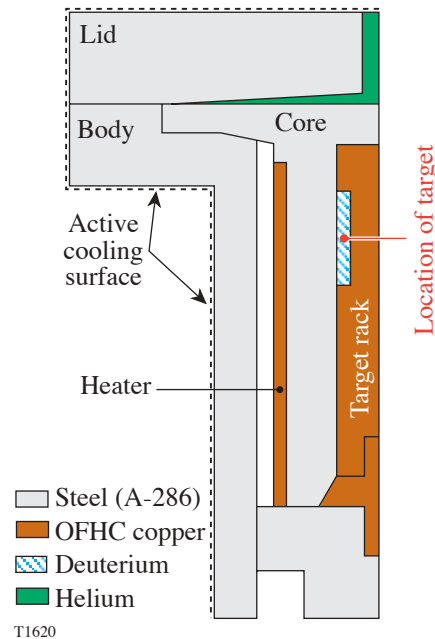
Figure 94.55 Pressure differential across an elastic capsule (GDP) wall of 1- μm thickness and 920- μm diameter, and a room-temperature volume of 0.17 cc. The capsule's buckling pressure (dashed line) is also plotted. While the maximum external pressure is reduced by more than a factor of 3 from the case of the inelastic shell (Fig. 94.53), the capsule's buckling pressure would still be exceeded.

Modeling the Transient Cooling Phase

A computational fluid dynamics (CFD) program is used to calculate the temperature profiles and heat flows inside the permeation cell. Only through modeling can the thermal conditions and the forces on the capsule during the transient cooling phase be quantified. When cooling is enacted, the thermal gradients change inside the permeation cell and therefore across the capsule wall. This temperature difference creates a pressure difference that leads to either a burst or buckling pressure on the capsule. Exceeding the material properties causes the capsule to fail by either bursting or collapsing. As stated previously, the failure pressure of thin-walled capsules is small, and significant pressure differences can occur during transient cooling processes if the cooling rate

is too large. The CFD simulation is used to calculate the resulting pressure difference across the capsule wall caused by cooling steps throughout the temperature range from 294 K to 40 K. These results are used to determine a cooling program that could successfully cool capsules until the fuel freezes while avoiding a pressure difference that may destroy the capsule. Reducing the typically lengthy cooling time increases target production and saves operator effort. A maximized cooling rate is much more important when filling with DT; reducing the cooling time will minimize He³ buildup and capsule deterioration.

The permeation cell and its components are recreated as a two-dimensional axisymmetric model, shown in Fig. 94.56. The model is comprised of the A-286 superalloy body, lid, and core, the copper target rack, and deuterium gas in the space



T1620

Figure 94.56 A two-dimensional axisymmetric representation of the permeation cell. The properties of the temperature-dependent materials are accounted for in the model. The capsule is located in the center of the gas space around the target rack. The boundary conditions are held on the outer cooling surfaces of the model, and the temperatures are implemented by changing the power to the heater. The averages gas temperatures external and internal to the capsule wall are recorded. The corresponding external and internal pressures, which are a function of temperature and density, are calculated from the deuterium equation of state.

surrounding the capsule and target rack. The capsule is located in the center of the deuterium gas space in the notch of the target rack. The solutions are generated using *FLUENT* computational fluid dynamics software.¹³

The following solution procedure is used to determine the pressure difference across the capsule wall. Temperature boundary conditions are set on the outer surfaces of the model (on the lid and body) and on the heater, as shown in Fig. 94.56. The permeation cell is initially considered isothermal. This assumption is applicable for deuterium—not DT, which generates heat—and is an approximation of the actual conditions. The solver uses the temperature-dependent material properties of the components and gas, which are listed in Table 94.I. These properties span a wide range over the temperature range from 294 K to 40 K. To commence the simulation, the temperature setting on the silicon diode is lowered to enact a cooling step. The temperature in each volume element is recorded as the simulation progresses, and a temperature profile in the permeation cell is generated. The simulation is run until a steady-state final temperature profile develops. This is assumed when the average capsule temperature reaches a steady value. From the instantaneous temperature in each volume element of the model, the time instantaneous and volume-averaged temperatures on either side of the capsule wall are calculated. These average temperatures are converted into average gas pressures from the deuterium equation of state. The average internal and external pressures of the capsule yield the bursting pressure as a function of time.

Cooling steps in increments of 0.125, 0.5, and 1 K are performed at temperatures through the temperature range from 294 K to 40 K. The size of the increments was chosen due to the accuracy of the sensors and the magnitude of actual cooling increments. (The temperature resolution of the sensor is 1 K at

300 K and 0.5 K at 100 K.) After a cooling step is made, the temperature of the gas inside the capsule lags behind that of the external gas and the magnitude of the difference depends on the temperature-dependent physical properties of the gas. The thermal diffusivities of the steel and deuterium are plotted in Fig. 94.57. The gas, which has a thermal diffusivity one to two orders of magnitude less than that of the metals, responds more slowly to temperature changes, and the difference increases at lower temperatures. The difference (ΔT) between the average external (to the capsule) and internal temperatures for three

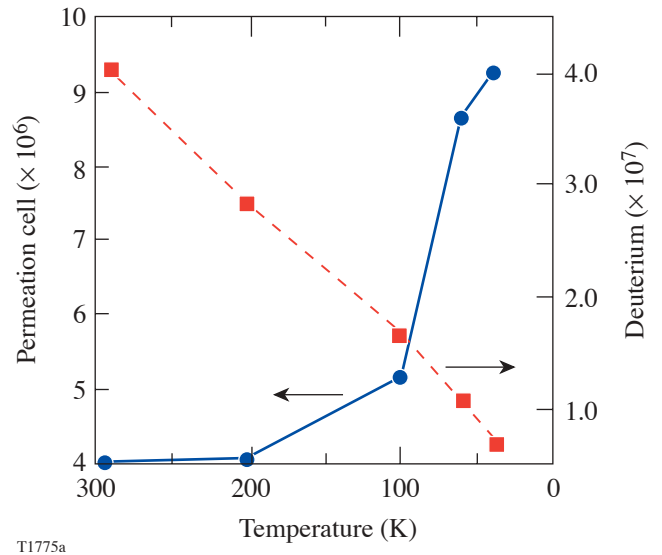


Figure 94.57 The thermal diffusivities of the steel and deuterium as a function of temperature are plotted. The gas, which has a thermal diffusivity one to two orders of magnitude less than that of the metals, responds more slowly to temperature changes, and the difference between the thermal diffusivity of the gas and steel increases at lower temperatures.

Table 94.I: Temperature-dependent properties of materials in the permeation cell model.

	294 K		100 K		40 K	
	C_p	k	C_p	k	C_p	k
Steel	503	16.3	216	9	40	3
Copper	381	388	253	500	60	1000
Deuterium (1000 atm @ 294 K)	7790	0.32	8900	0.15	14300	0.098
C_p = heat capacity (J/kg K) k = thermal conductivity (W/m K)						

different cooling steps is shown as a function of time in Figs. 94.58(a)–94.58(c). The largest average ΔT of about -0.2 K for a temperature change of 1.0 K occurs about 10 to 20 s after the change is made, depending at which temperature it occurs. As the temperature of the gas external to the capsule equilibrates, ΔT approaches zero in less than 100 s. The values of ΔT shown in the figures are negative for the case of cooling. It is possible, however, that ΔT becomes positive if the permeation cell was warmed (for example, a cooling power fluctuation or a control error).

The calculated temperature profiles are converted to pressure differences (ΔP) across the capsule wall. For temperature changes made in increments of 0.125 , 0.5 , and 1.0 K, the temporal pressure difference at temperatures through the cooling cycle are shown in Figs. 94.59(a)–94.59(c), respectively. Since the external temperature is less than the internal temperature, and likewise for the pressures, a burst pressure develops inside the capsule. The pressure gradient reaches a maximum ΔP_{\max} before dissipating as the temperatures across the wall equilibrate and/or permeation takes place. In all three cases, more severe pressure gradients occur at lower temperatures. This is explained by the increase of heat capacity and decrease of thermal conductivity of deuterium at reduced temperatures. The gas responds more slowly to thermal changes as the thermal diffusivity decreases. Therefore, as the difference

between the external and internal temperatures increases, so does the pressure difference. As shown, the induced burst pressure approaches 0.9 atm for a temperature change of 1.0 K. This is well within the limits of thin-walled plastic capsules. As mentioned in the previous paragraph, it is possible that ΔP becomes positive if the permeation cell was warmed. If this occurs, a buckling pressure would be applied on the capsule. For a $1\text{-}\mu\text{m}$ -wall GDP capsule, P_{buckle} is ~ 0.1 to 0.2 atm, and a warming of 0.125 K causes a buckling pressure very near the failure limit. It is therefore essential that $1\text{-}\mu\text{m}$ capsules are not warmed suddenly by more than 0.1 K.

No single cooling step of 1.0 K causes a pressure difference that would burst a capsule of these dimensions. A series of temperature changes, however, in which the next step occurs before the pressures equilibrate can cause ΔP to exceed its bursting pressure. After each cooling step, an amount of time elapses before ΔP vanishes due to temperature equilibration (assuming no permeability). The equilibration times, shown in Fig. 94.60, increase at the colder temperatures of the cooling program. This effect is also attributed to a lower thermal diffusivity of the gas. This suggests that greater consideration must be taken in this temperature regime, namely a slower cooling rate. Likewise, the cooling rate (and associated depressurization rate) may be increased in the initial stages of the cooling program where temperatures are higher.

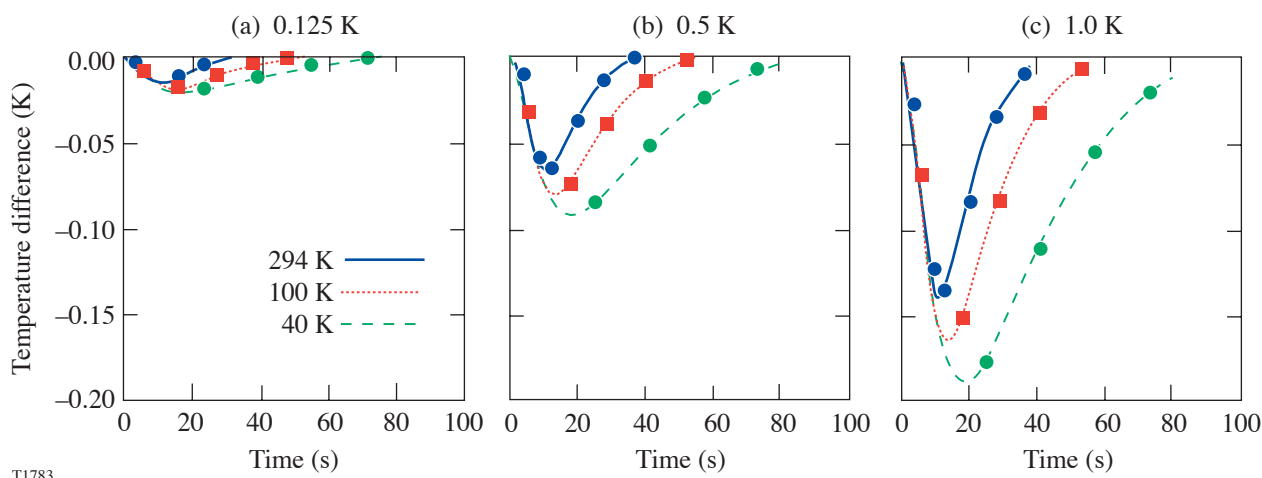


Figure 94.58

The difference (ΔT) between the average external (to the capsule) and internal temperatures for cooling steps of (a) 0.125 K, (b) 0.5 K, and (c) 1.0 K is plotted as a function of time for various temperatures. The largest average ΔT of nearly -0.2 K for a temperature change of 1 K occurs about 10 to 20 s after the change is made, depending at which temperature it occurs. As the temperature of the gas external to the capsule equilibrates, ΔT approaches zero in less than 100 s. The values of ΔT shown in the three figures are negative for the case of cooling. It is possible, however, that ΔT becomes positive if the permeation cell was warmed.

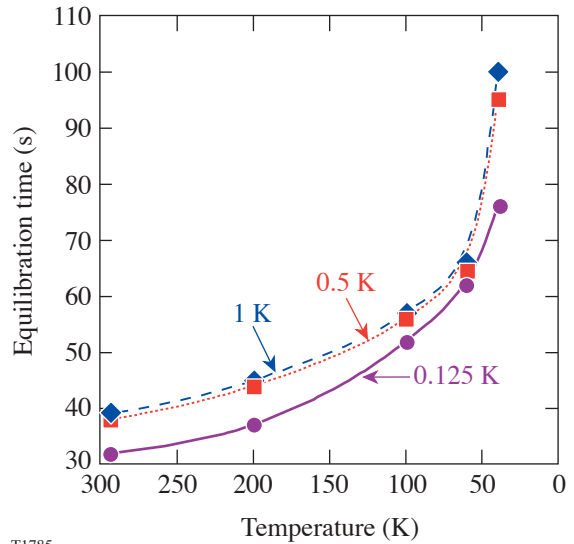
The permeability of the capsule material affects the pressure gradients across its wall. As time elapses, the pressure difference between the external and internal gas will be reduced as the temperatures equilibrate and permeation occurs. Permeation through a polystyrene capsule is temperature dependent and permeability follows the Arrhenius relation:⁹

$$K_p = 1.18 \times 10^{-12} \exp(-1535/T),$$

where K_p is in units of mol/m s Pa and T is in K. The permeation time constant τ of deuterium through polystyrene is given by the equation

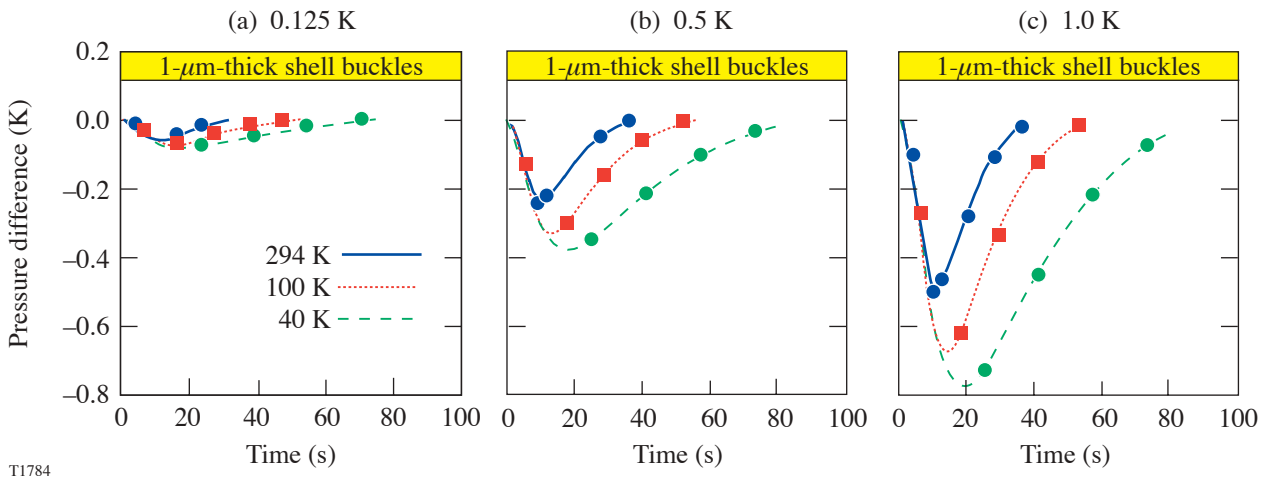
$$\tau = wD/6 K_p RT,$$

where w and D are the capsule's wall thickness and diameter, respectively, and R is the gas constant. (Vapor-deposited polyimide capsules can be less permeable.) Since the gas outside the capsule cools first and reduces pressure, an overpressure inside the capsule occurs for each temperature change. A succession of cooling steps can be viewed as a depressurization rate on the capsule. The maximum-allowable depressurization rate a capsule may experience is expressed as



T1785

Figure 94.60 The amount of time required for the pressure difference to equilibrate across the capsule wall after a cooling step, assuming no permeation, as a function of temperature. Curves for the three different cooling steps are shown. The time increases at lower temperatures due to the increase in thermal diffusivity of the gas.



T1784

Figure 94.59 The difference (ΔP) between the external (to the capsule) and the internal gas pressures that arise from cooling steps of (a) 0.125 K, (b) 0.5 K, and (c) 1.0 K is plotted as a function of time for various temperatures. Negative values of ΔP indicate a burst pressure. The external and internal gas pressures, which are a function of temperature and density, are calculated from the deuterium equation of state. The peak ΔP occurs at 10 to 20 s and is more pronounced at lower temperatures. The values of ΔP shown in the three figures are negative for the case of cooling. It is possible, however, that ΔP becomes positive (representing a buckling pressure) if the permeation cell was warmed. The dashed line indicates the value of ΔP at which a 1- μ m-wall GDP capsule will buckle. Capsules with a 1- μ m-thick wall would easily buckle from positive temperature changes of 0.5 K and 1 K and are near the limit for temperature changes of 0.125 K.

$\sim (P_{\text{burst}}/\tau)$, where P_{burst} is the capsule's bursting pressure. The capsule would fail if the bursting pressure was reached while depressurizing at this rate. Assuming a 920- μm -diam capsule with a 3- μm -thick wall and material properties of GDP, the capsule's bursting pressure is ~ 5.7 atm. Since τ is inversely proportional to temperature and permeability, the maximum-allowable depressurization rate decreases at lower temperatures; thus, cooling should be slowed to prevent capsule breakage. A plot of allowable depressurization rates (dP^*/dt) is shown in Fig. 94.61, where, as a safety concern, (dP^*/dt) is one-half the maximum value. At the temperature at which the capsule becomes impermeable, (dP^*/dt) approaches zero because τ approaches infinity. However, low depressurization rates (~ 0.1 K/min) are possible because the capsule never reaches P_{burst} before the pressures are balanced by temperature equilibration.

Currently, gas-filled capsules are cooled at a rate of 0.1 K/min from room temperature until the fuel liquefies. Thus, it takes about 45 h to complete the process. A faster cooling program may be achieved by analyzing the pressure differ-

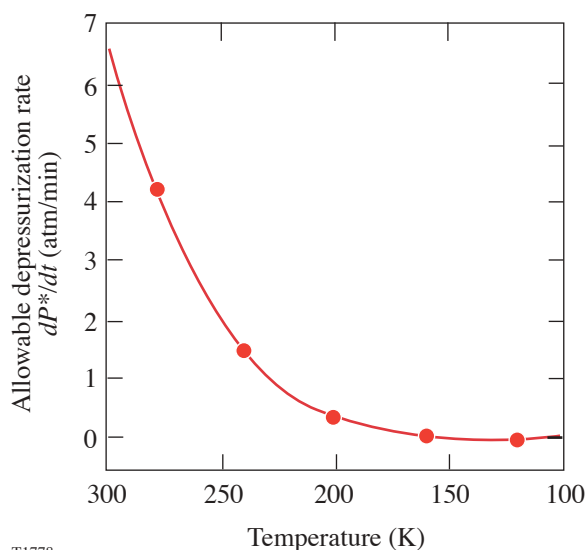
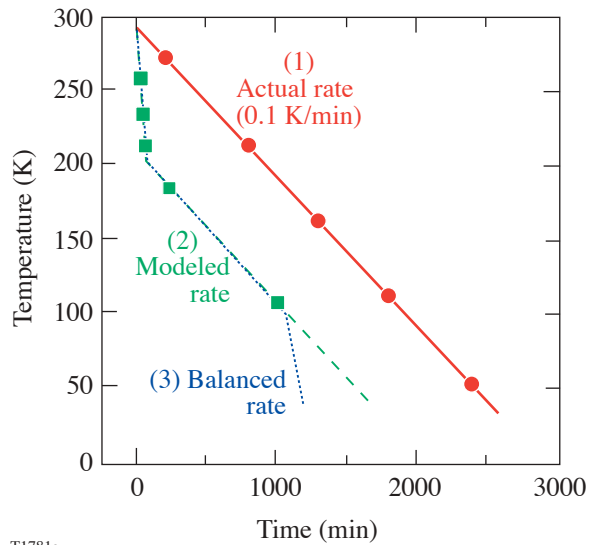


Figure 94.61

Allowable depressurization rates (dP^*/dt) for a 920- μm -diam, 3- μm -thick-wall capsule as a function of temperature. The allowable rate was one-half the maximum rate for safety considerations. The curve is based on the relationship $(dP/dt) \sim (P_{\text{burst}}/\tau)$. The permeability values of polystyrene were used to calculate τ because the temperature-dependent permeability of GDP has not been measured. This approximation is used because of the generally similar Arrhenius behavior of polymers and the similar values of permeability of polystyrene and GDP at room temperature.

ences on the capsule via modeling. From the cooling-induced pressure differences shown in Figs. 94.59(a)–94.59(c), the maximum pressure difference occurs ~ 10 to 20 s after the cooling step. From the initial descent portion of each curve (until ΔP_{max}), one can calculate the depressurization rate of the gas outside the capsule that arises from a temperature change. The goal then is to make cooling steps that maintain the depressurization rate below the allowable value (dP^*/dt) shown in Fig. 94.61 at each temperature. As shown in Fig. 94.59(c), from 294 K to 255 K, a cooling step of 1 K can be made, which results in ΔP_{max} of 0.48 atm in 10 s. This gives a depressurization rate of 2.9 atm/min, which can be converted back into a cooling rate. To minimize the total cooldown time, a subsequent cooling step should be made at the time ΔP_{max} is reached, about 10 s for the 294-K curve in Fig. 94.59(c). Thus a cooling rate of 5 K/min can be performed safely. According to Fig. 94.61, in the temperature range from 255 K to 240 K, it is required that (dP^*/dt) be less than ~ 2 atm/min. From the 294-K curve in Fig. 94.59(b), a cooling step of 0.5 K causes ΔP_{max} of 0.24 atm at 11 s. The use of the 294-K curve at these temperatures is justified because the initial slopes of the 294-K and 200-K curves (the latter is not shown) that cover this temperature range are essentially similar. This corresponds to a depressurization rate of 1.31 atm/min, which is safely within the limit. If another cooling step is made at 11 s (the time when ΔP_{max} is reached), then the subsequent cooling rate is 2.7 K/min. This procedure was continued in a likewise fashion to further choose temperature changes below 240 K that maintain the depressurization rate below (dP^*/dt) as cooling progresses. These calculations yield an acceptable cooling program to 40 K, shown in Fig. 94.62, where the minimum rate of 0.1 K/min is used below 200 K. For comparison, the cooldown program used in actual experiments of 0.1 K/min throughout the entire temperature range from 294 K to 40 K is also plotted in the figure. With the revised cooling program, which takes into account permeation at higher temperatures, the total cooling time has dropped from 2450 min to 1670 min, a savings of over 14 h (34% of the total time).

When considering the buckling pressure caused by the steady-state effects described earlier (thermal contraction mismatch and room-temperature gas volume) and the burst pressure caused by transient cooling, it is conceivable that one could balance these contributions to develop a faster cooling program. Note that capsules are more susceptible to buckling than bursting. As shown in Fig. 94.55, a dangerous buckle pressure of about 0.2 to 0.5 atm arises while cooling from 100 K to 50 K. In this regime, a cooling step of 0.5 K, which causes a burst pressure of about 0.3 atm, may be used to offset



T1781a

Figure 94.62

Temperature program for cooling a gas-filled capsule to freezing. Three different programs are plotted: (1) the currently used experimental rate (0.1 K/min), (2) a faster rate that accounts for permeation at higher temperatures to offset pressure differences, and (3) a proposed faster rate that accounts for permeation at higher temperatures and allows cooling-induced burst pressures and steady-state-effect buckle pressures to counterbalance each other.

buckling pressure. If a step is made every minute, allowing for the pressure to equilibrate, it is plausible that the total cooling time may be halved to ~ 1200 min, as shown in Fig. 94.62.

Summary

An analysis of the temperature and pressure gradients in the permeation cell that occur during the cooling of thin-walled cryogenic targets has been presented. Both steady-state and transient effects may cause the capsule to fail during cooling. The steady-state contribution to the pressure difference arises from three sources: (1) the thermal contraction of the materials that comprise the capsule and the permeation cell, (2) the room-temperature volume of gas in the line connecting the permeation cell to the isolation valve, and (3) elastic deformation of the capsule. An optimum value for the room-temperature volume has been found that minimizes the burst and buckle pressures. The transient analysis considered the pressure differences across the capsule wall that arise from temperature changes to the permeation cell. A $3\text{-}\mu\text{m}$ -wall capsule can withstand changes of 1 K at warmer temperatures, while a $1\text{-}\mu\text{m}$ -wall capsule should not be subjected to sudden temperature changes of more than 0.1 K. A cooling program that incorporates permeability at higher temperatures and safely

maintains the capsule within the critical burst and buckle pressures allows the time to reach the frozen state to be reduced by over 30%.

ACKNOWLEDGMENT

This work was supported by the U.S. Department of Energy Office of Inertial Confinement Fusion under Cooperative Agreement No. DE-FC03-92SF19460, the University of Rochester, and the New York State Energy Research and Development Authority. The support of DOE does not constitute an endorsement by DOE of the views expressed in this article.

REFERENCES

1. Laboratory for Laser Energetics LLE Review **90**, 49, NTIS document No. DOE/SF/19460-437 (2002). Copies may be obtained from the National Technical Information Service, Springfield, VA 22161.
2. D. D. Meyerhofer, C. Chiritescu, T. J. B. Collins, J. A. Delettrez, R. Epstein, V. Yu. Glebov, D. R. Harding, R. L. Keck, S. J. Loucks, L. D. Lund, R. L. McCrory, P. W. McKenty, F. J. Marshall, S. F. B. Morse, S. P. Regan, P. B. Radha, S. Roberts, W. Seka, S. Skupsky, V. A. Smalyuk, C. Sorce, C. Stoeckl, J. M. Soures, R. P. J. Town, J. A. Frenje, C. K. Li, R. D. Petrasso, F. H. Séguin, K. Fletcher, C. Padalino, C. Freeman, N. Izumi, R. Lerche, T. W. Phillips, and T. C. Sangster, presented at the 14th Target Fabrication Meeting, West Point, NY, 15–19 July 2001.
3. Laboratory for Laser Energetics LLE Review **81**, 6, NTIS document No. DOE/SF/19460-335 (1999). Copies may be obtained from the National Technical Information Service, Springfield, VA 22161.
4. M. D. Wittman, D. R. Harding, P. W. McKenty, H. Huang, L. S. Iwan, T. J. Kessler, L. Elasky, and J. Sailer, presented at the 14th Target Fabrication Meeting, West Point, NY, 15–19 July 2001.
5. S. G. Noyes, M. J. Bonino, D. Turner, J. Tidu, and D. R. Harding, presented at the 14th Target Fabrication Meeting, West Point, NY, 15–19 July 2001.
6. A. Nikroo *et al.*, *Fusion Sci. Technol.* **41**, 214 (2002).
7. R. Prydz, K. D. Timmerhaus, and R. B. Stewart, in *Advances in Cryogenic Engineering*, edited by K. D. Timmerhaus (Plenum Press, New York, 1968), Vol. 13, pp. 384–396.
8. G. K. White, *Experimental Techniques in Low-Temperature Physics*, 2nd ed., Monographs on the Physics and Chemistry of Materials (Clarendon Press, Oxford, 1968), p. 377.
9. L. A. Scott, R. G. Schneggenburger, and P. R. Anderson, *J. Vac. Sci. Technol. A* **4**, 1155 (1986).
10. F.-Y. Tsai, D. R. Harding, S. H. Chen, T. N. Blanton, and E. L. Alfonso, *Fusion Sci. Technol.* **41**, 178 (2002).
11. R. Stephens, General Atomics, private communication (2001).
12. W. C. Young, in *Roark's Formulas for Stress & Strain*, 6th ed. (McGraw-Hill, New York, 1989), p. 523.
13. *FLUENT* (version 6.0.20), Fluent USA Inc., Lebanon, NH 03766.

